Microporous and Mesoporous Materials 268 (2018) 50–57

Contents lists available at ScienceDirect

Microporous and Mesoporous Materials

journal homepage: www.elsevier.com/locate/micromeso

Adjusting the proportions of extra-framework K^+ and Cs^+ cations to construct a "molecular gate" on ZK-5 for CO_2 removal

Jiangfeng Yang[a,c], Hua Shang[a], Rajamani Krishna[b], Yong Wang[c], Kun Ouyang[a], Jinping Li[a,c,*]

[a] Research Institute of Special Chemicals, College of Chemistry and Chemical Engineering, Taiyuan University of Technology, Taiyuan 030024, Shanxi, PR China
[b] Van 't Hoff Institute for Molecular Sciences, University of Amsterdam, Science Park 904,1098 XH Amsterdam, The Netherlands
[c] Shanxi Key Laboratory of Gas Energy Efficient and Clean Utilization, Taiyuan 030024, Shanxi, PR China

ARTICLE INFO

Keywords:
Zeolite
ZK-5
Adsorption
Molecular gate
CO_2

ABSTRACT

For the capture of CO_2 from flue gas and decarbonization of natural gas streams, an ideal adsorbent should have a high selectivity for CO_2 over N_2 and CH_4. In this work, through adjusting the proportions of extra-framework K^+ and Cs^+ cations and varying the Si/Al ratios of the zeolite ZK-5, the small "molecular gate" adsorbent ZK-5-*n*-K has been prepared. An increase in the number of K^+ cations prevents the ingress of the larger molecules CH_4 and N_2, while allowing entry of the smaller CO_2; the net result is that CO_2 capture from CH_4 or N_2 is achieved with unusually high selectivity, of the order of 1×10^5. Grand canonical Monte Carlo simulations show that the extra-framework K^+ and Cs^+ cations are positioned at different locations in the ZK-5; K^+ locates near the 8-ring window, whereas Cs^+ resides in the interior regions. The separation performances of 12 different K^+- and Cs^+-doped ZK-5 structures (with four different Si/Al ratios of 3.17, 3.36, 3.46, and 3.57) have been investigated. Transient breakthrough simulations have been used to quantify the CO_2 capture performances in four sets of separations: 30%/70%, 5%/95%, and 2%/98% CO_2/CH_4 mixtures at a total pressure of 1 MPa, and a 15%/85% CO_2/N_2 mixture at a total pressure of 100 kPa. In all cases, the selectivities were sufficiently high to ensure that the separation performance was primarily governed by the CO_2 uptake capacity. The overall conclusion to be drawn from this work is that ZK-5 is a suitable adsorbent for the decarbonization of natural gas.

1. Introduction

In view of environmental concerns, the capture and storage of CO_2 is becoming of increasing industrial and societal importance [1]. Of particular importance is CO_2 capture from the flue gas (15%/85% CO_2/N_2) emanating from electric power plants; this accounts for more than 35% of global carbon emissions [2]. CO_2 separation from CH_4 is important in natural gas processing because CO_2 reduces the energy content of natural gas [3–5]. The current technology used for CO_2 involves absorption by amine solutions, but this is energy-intensive [6]. Pressure-swing adsorption (PSA) using a fixed bed containing a solid adsorbent material offers an energy-efficient alternative to amine absorption technology [7–9].

For the capture of CO_2 from flue gas and natural gas streams, an ideal adsorbent should have a combination of high CO_2 working capacity, high selectivity for CO_2 over N_2 and CH_4, and high stability and sustainability. Porous solid materials, including zeolites [10–13], anodic aluminum oxide [14], active carbon materials [15–18], polymers [19], and metal–organic frameworks (MOFs) have been investigated as possible adsorbents [20–22]. Of all potential adsorbents, zeolites possess chemical and thermal stability, and are moderately inexpensive [23]. Of particular potential interest are zeolite adsorbents that are endowed with "molecular gate" or "molecular trapdoor" capabilities, allowing effective separation of $CO_2/CH_4/N_2$mixtures with kinetic diameters that are close to one another:3.3, 3.8, and 3.64 Å, respectively [8,24–27]. Kuznicki et al. reported the first such "molecular gate" material, ETS-4, with adjustable pores for size-selective adsorption of molecules; this titanosilicate can be systematically contracted through dehydration at elevated temperatures to "tune" the effective size of the pores, allowing access to the interior of the crystal [24]. This "molecular gate" effect can be used to tailor the adsorption properties of the materials to give size-selective adsorbents suitable for commercially important separations of gas mixtures of molecules of similar size in the range 3.0–4.0 Å, such as those of N_2/CH_4, Ar/O_2, and N_2/O_2. Shang et al. reported Cs-CHA (chabazite) with a "molecular trapdoor" effect, which showed record high selectivities for the separation of important industrial gas mixtures, such as CO_2/CH_4, because the gas molecules have sufficient interaction ability to induce the

* Corresponding author. Research Institute of Special Chemicals, College of Chemistry and Chemical Engineering, Taiyuan University of Technology, Taiyuan 030024, Shanxi, PR China.
E-mail address: jpli211@hotmail.com (J. Li).

https://doi.org/10.1016/j.micromeso.2018.03.034
Received 2 February 2018; Received in revised form 11 March 2018; Accepted 29 March 2018
Available online 30 March 2018
1387-1811/

"door-keeping" cations to deviate from the center of pore apertures [26]. CHA has 8-ring windows of dimensions 3.8 Å × 3.8 Å, too close to the kinetic diameter of CH_4, and so a few large Cs^+ cations can stop the infusion of CH_4 into its structure. This phenomenon is different from that of the large pore size LTA (4.2 Å × 4.2 Å) and FAU (7.4 Å × 7.4 Å) zeolites (NaKA and 13×) [12,13], which need more and vary cations located in the structure to stop CH_4 diffusion in, obviously, that was harder to construction.

Zeolite KFI, has8-ring windows of dimensions 3.9 Å × 3.9 Å, slightly larger than CHA but much smaller than LTA and FAU, so its separation performance can be tuned easily by adjusting the proportions of extra-framework Li^+, Na^+, K^+, Cs^+, Ga^{3+}, and Mg^{2+} cations [28–33]. Thus, the "molecular gate" phenomenon can be expected in KFI-type zeolites (ZK-5). However, a high Si/Al ratio (Si/Al > 3.60) in such samples allows both CO_2 and CH_4 to readily diffuse through the structure. Although a low Si/Al ratio (Si/Al = 1.67) in such samples has a profound influence on the pore volume and CO_2 adsorption characteristics, a significant gas "molecular gate" effect has not yet been demonstrated [28,33]. In our investigations, a K^+-doped zeolite ZK-5-K (Si/Al = 3.17) has been prepared that clearly exhibits the "molecular gate" effect, resulting in ultra-high CO_2 selectivity. The separation performances of 12 different ZK-5 structures with varying Si/Al ratios and varying proportions of extra-framework K^+ and Cs^+ cations have been investigated. Specifically, the following four sets of separations have been examined: 2%/98%, 5%/95%, and 30%/70% CO_2/CH_4 mixtures at a total pressure of 1 MPa, and a 15%/85% CO_2/N_2 mixture at a total pressure of 100 kPa.

2. Experimental

2.1. Materials

ZK-5 (Cs/K) was synthesized with a gel composition of $2.4K_2O{:}0.06Cs_2O{:}nSiO_2{:}Al_2O_3{:}36H_2O$ [34] ($8.8 < n < 11.6$). The typical procedure involved mixing of the required amounts of KOH and water in a PTFE bottle, heating at 373 K for 10 min to obtain a clear solution, followed by addition of $Al(OH)_3$. The resulting clear solution was heated under reflux for a further 10 min at 373 K, then allowed to cool to room temperature. CsOH was then added to the above clear solution at room temperature, and the silica sol was added with stirring over a period of 10 min. Finally, the resultant mixture was transferred to a Teflon-lined autoclave and heated in an oven for 4 days at 393 K. After cooling to ambient temperature, the obtained product was collected by filtration, washed three times with water, and dried in an oven at 358 K. The crystal structure of KFI and the degree of crystallinity were confirmed by powder XRD.

2.2. Ion-exchange

ZK-5, obtained as described above, was converted from its cesium form (K/Cs-ZK-5). Typically, 1 M KCl (200 mL) was added to zeolite (5 g), and the mixture was heated to 353 K and stirred for 12 h. The supernatant was then decanted off and continuously replaced by water to keep the level unchanged. After successive washes with the required solution, the resulting zeolite was collected by vacuum filtration and washed with deionized water (500 mL). The zeolite was then dried at 373 K for 24 h; it was designated as ZK-5-K.ZK-5-Cs was prepared from K/Cs-ZK-5 by ion-exchange of ZK-5 with 1 M CsCl (5 g zeolite:200 mL aqueous CsCl) by a process similar to that described for ZK-5-K.

2.3. Characterization

The crystallinity and phase purity of the molecular sieves were measured by powder XRD using a Rigaku Mini Flex II X-ray diffractometer with Cu-K_α radiation operated at 30 kV and 15 mA. The scanning range was from 5 to 40° (2θ) at 1°/min. Morphological data were acquired by scanning electron microscopy (SEM) using a Hitachi SU8010 instrument operated at 2.0 kV or 20.0 kV. The samples were coated with gold to increase their conductivity before scanning. TGA was carried out in a flowing atmosphere (argon flow rate: 100 mL/min) at a heating rate of5 K/min using a Netzsch STA-409-C balance. The Si/Al ratio and the cation content of the zeolites were determined by elemental analysis using a Varian 723P spectrophotometer (Table S1).

2.4. High-pressure gas adsorption measurements

The purities of the carbon dioxide, methane, and nitrogen used were 99.999%, 99.95%, and 99.999%, respectively. The adsorption isotherms were measured under high pressure (up to 1 MPa) using an Intelligent Gravimetric Analyzer (IGA 001, Hiden, UK). Before measuring each isotherm, a 30–50 mg sample was pre-dried under reduced pressure and then outgassed overnight at 423 K under high vacuum (1×10^{-4} Pa) until no further weight loss was observed. Each adsorption step was allowed to approach equilibrium over a period of 60 min, and all of the isotherms for each gas were measured using a single sample.

3. Calculations and simulation

3.1. Details of GCMC calculations

Grand canonical Monte Carlo (GCMC) simulations using the Sorption code in Materials Studio [35] were performed to study the positions of K^+ or Cs^+ in the ZK-5 structure. We assumed "adsorption" of K^+ and Cs^+ on the zeolite. The ZK-5 framework was treated as rigid, with atoms frozen at their crystallographic positions during GCMC simulations. A simulation box containing 8 (2 × 2 × 2) unit cells, with periodic boundary conditions applied in all three dimensions, was built in this work. A cut-off radius was set at 12 Å for LJ interactions, and long-range electrostatic interactions were handled using the Ewald summation method. For each state point, GCMC simulation comprised 2.0×10^7 steps to guarantee equilibration, followed by 2.0×10^7 steps to sample the desired thermodynamic properties. All potential parameters for the atoms in ZK-5 and for K^+ and Cs^+ were taken from the COMPASS force field.

3.2. Fitting of experimental data on pure component isotherms

The experimental unary isotherm data for CO_2, CH_4, and N_2 at 298 K in ZK-5 zeolite, with varying Si/Al ratios, and varying proportions of extra-framework cations, K^+ and Cs^+, were fitted with the Langmuir–Freundlich model:

$$q = q_{sat}\frac{bp^v}{1 + bp^v} \tag{1}$$

The fitted Langmuir–Freundlich parameters for CO_2, CH_4, and N_2 are presented in Table S2, Table S3, and Table S4, respectively.

3.3. Ideal adsorbed solution theory (IAST)calculations of adsorption selectivities and uptake capacities

The selectivity of preferential adsorption of component i over component j can be defined as:

$$S_{ads} = \frac{q_i/q_j}{p_i/p_j} \tag{2}$$

In Equation (2), q_i and q_j are the uptake capacities in the adsorbed phase, expressed in mol kg^{-1}. We report the uptake capacities in terms of mol L^{-1} of adsorbent, obtained by multiplying the gravimetric uptake capacities by the framework density, expressed in kg L^{-1}; the framework densities are provided in Table S1.

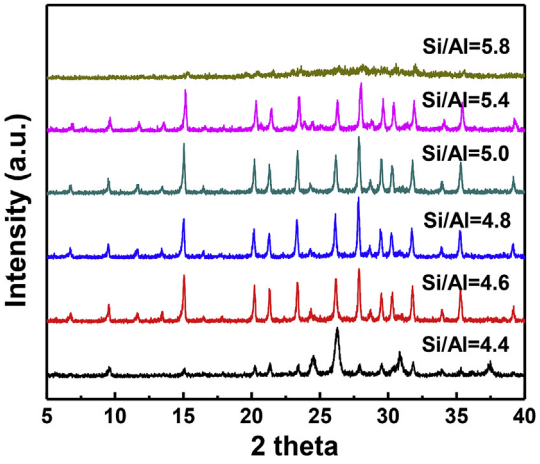

Fig. 1. Effect of Si/Al in raw materials on synthesized ZK-5.

3.4. Transient breakthrough simulations

Fixed beds, packed with crystals of microporous materials, are commonly used for the separation of mixtures; such adsorbers are commonly operated in transient mode, and the compositions of the gas phase and component loadings within the crystals vary with position and time. During the initial stages of the transience, the pores are gradually loaded, and only towards the end of the adsorption cycle do conditions correspond to pore saturation. For a given separation task, transient breakthroughs provide a more realistic evaluation of the efficacy of a material, as they reflect the combined influence of adsorption selectivity and adsorption capacity. The breakthrough simulation methodology used here was the same as that used in our previous publications [36–38].

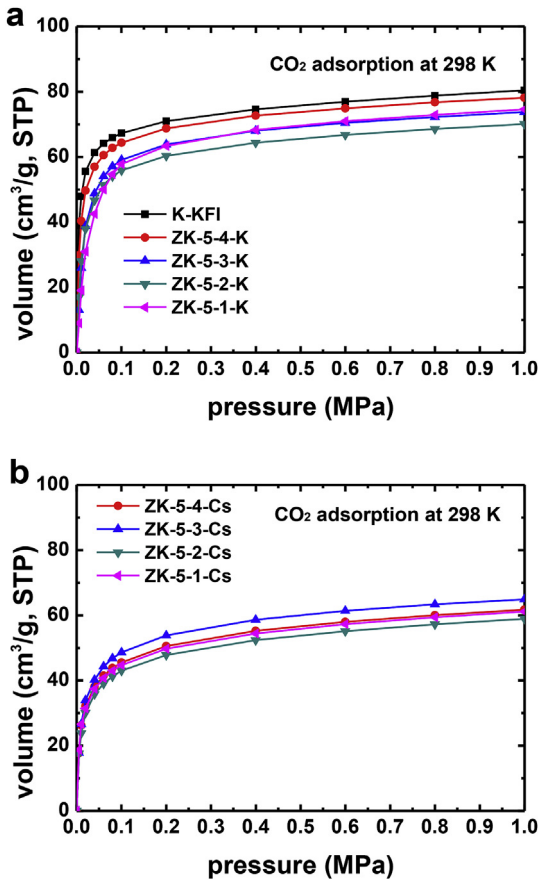

Fig. 2. CO_2 adsorption on K-KFI, ZK-5-N-K (a) and ZK-5-N-Cs (b) at 298 K and the pressure up to 1 MPa.

4. Results and discussion

Different Si/Al ratios will impart the porous zeolite with various functions and properties. Here, it was found that ZK-5 crystals could be successfully grown at Si/Al ratios in the range 4.6–5.4 (Fig. 1). A higher ratio decreased the XRD peaks. In order to investigate the influence of extra-framework cations, ZK-5 samples with four different Si/Al ratios (4.6, 4.8, 5.0, and 5.4) were prepared. These were designated as ZK-5-1/2/3/4 (Fig. S1). Elemental analysis gave Si/Al ratios of 3.17, 3.36, 3.46, and 3.57 for ZK-5-1, ZK-5-2, ZK-5-3, and ZK-5-4, respectively, with K/Cs = 40%/60% (Table S1). Cs^+- and K^+-modified ZK-5 samples were prepared by ion-exchange in 1 M CsCl or KCl solution, respectively; the quantities exchanged were about 90% (K/Cs = 1:9 or 9:1), and the resulting samples were designated as ZK-5-1/2/3/4-Cs and ZK-5-1/2/3/4-K (Fig. S1). Structural formulae of the ZK-5 samples for one unit cell were determined on the basis of elemental analysis results, and are shown in Table S1 ($O_{192}Al_{(21-23)}Si_{(73-75)}K_nCs_{((21-23)-n)}$). The density of each sample was calculated from the quality and volume of one unit cell. As cesium has an atomic weight of 133 compared to 39 for potassium, the densities of ZK-5-*n*-Cs (*n*: 1/2/3/4) were higher than those of ZK-5-*n*-K (Table S1).

Since the surface area of ZK-5 cannot be measured from a liquid nitrogen adsorption isotherm [33], the surfaces of all samples were analyzed by measuring CO_2 adsorption isotherms at 273 K (Figs. S2–S4). The microporous surface area was calculated using the Dubinin – Radushkevitch (D-R) equation [39,40]. ZK-5-*n* showed the highest surface area, followed by ZK-5-*n*-K and ZK-5-*n*-Cs (Tables S2–S4). All surface areas decreased with decreasing Si/Al ratio.

Fig. 2 shows the CO_2 adsorption isotherms of ZK-5-*n*-Cs and ZK-5-*n*-K samples up to 1 MPa. Although the adsorption capacities were similar for the respective samples, the CO_2 uptakes at 100 kPa were nevertheless dependent on the Si/Al ratio in ZK-5-K samples (K-KFI [33] has a higher Si/Al ratio of 4.58). A zeolite with a lower Si/Al ratio requires more balancing ions (a content of cations equal to the content of Al) within its structure, and excess K^+ was found to prevent the infusion of some CO_2 molecules. For the ZK-5-Cs samples, however, the CO_2 adsorption capacity was not affected by the Cs^+ content. In other words, although the Cs^+ cation is much larger than the K^+ cation, more Cs^+ does not prevent the infusion of CO_2 molecules, from which we preliminary surmise that K^+ and Cs^+ reside in different sites in the ZK-5 structure. Comparing the ZK-5-*n*-Cs and ZK-5-*n*-K samples, the former showed lower capacity based on mass, but the capacities based on volume ratios were very similar at pressures up to 1 MPa (Table 1, Fig. S1). From this, we surmise that the pore volume of ZK-5 samples does not significantly change when K^+ is replaced by Cs^+.

The diameter of a CO_2 molecule is only 3.3 Å, and so it can diffuse in and out of the 3.9 Å windows (eight-membered rings of KFI) without restriction, but the larger gas molecules N_2 and CH_4 cannot infuse so easily; their infusion is greatly affected by the Si/Al ratio (Fig. 3). Fig. 3a shows that more K^+ cations led to lower gas uptake, and an exponential change in N_2 adsorption capacity based on a small change in Si/Al ratio: 14.2 $cm^3\,g^{-1}$ for ZK-5-3-K, 25.95 $cm^3\,g^{-1}$ for ZK-5-4-K, and 31.39 $cm^3\,g^{-1}$ for K-KFI (Si/Al = 4.58), that is, a significant difference between the ZK-5-3-K and ZK-5-4-K samples. More interestingly, the N_2 uptake capacities of the ZK-5-Cs samples did not change, irrespective of the amount of Cs^+ based on the different Si/Al ratios. The significant differences in N_2 adsorption on ZK-5-*n*-K further support our conclusion that K^+ and Cs^+ reside in different sites in the ZK-5 structure. We assume that K^+ resides near the window of the eight-membered-ring opening, such that a small change in K^+ concentration will close or open molecular diffusion channels. Conversely, Cs^+ is adsorbed far from the windows, such that N_2 infusion is not affected by

Table 1
Adsorption capacity (volume ratio: v/v) of CO_2, CH_4 and N_2 on different Si/Al ratio ZK-5 samples at 1 and 1 MPa.

Material	Si/Al	CO_2 (v/v)		N_2 (v/v)		CH_4 (v/v)	
		100 kPa	1 MPa	100 kPa	1 MPa	100 kPa	1 MPa
ZK-5-1	3.17	130.65	164.04	9.85	54.22	20.83	67.92
ZK-5-1-K		101.18	130.60	4.2	31.27	4.94	24.05
ZK-5-1-Cs		97.47	133.24	12.38	55.59	19.21	64.59
ZK-5-2	3.36	121.19	154.74	9.89	53.37	15.99	60.07
ZK-5-2-K		98.94	124.09	5.36	30.00	6.27	25.65
ZK-5-2-Cs		93.31	127.92	11.80	52.80	21.90	70.31
ZK-5-3	3.46	128.54	161.06	14.07	53.69	20.50	53.91
ZK-5-3-K		104.05	129.82	4.52	24.90	6.78	21.79
ZK-5-3-Cs		105.08	140.21	11.38	54.11	13.93	54.19
ZK-5-4	3.57	128.41	162.87	14.43	55.03	21.01	55.26
ZK-5-4-K		117.05	139.91	9.61	46.45	14.57	53.74
ZK-5-4-Cs		97.48	132.08	10.74	51.27	12.73	50.91
K-KFI	4.58	120.57	144.20	12.43	54.62	30.49	74.30

a change in its concentration.

Based on this theory of balance ions closing the windows, larger molecules should be more adversely affected. Fig. 3c shows CH_4 adsorption isotherms on the ZK-5-K samples. It can be further inferred that more K^+ balance ions close the windows of the channels; ZK-5-1-K, with the lowest Si/Al ratio, showed a CH_4 adsorption capacity of 7.85 $cm^3\,g^{-1}$, as compared to 42.70 $cm^3\,g^{-1}$ for K-KFI with the highest Si/Al ratio. Thus, an increase in Si/Al ratio from 3.17 to 4.58 led to a more than fivefold increase in capacity. As for N_2 adsorption, there was a significant difference between ZK-5-3-K and ZK-5-4-K, implying an inflection point between these two samples. Considering all of the CO_2, N_2, and CH_4 adsorption isotherms on the ZK-5-K samples, it can be concluded that adsorption of more K^+ on the KFI-type structure will close the eight-membered-ring windows, limiting the infusion of larger molecules, thereby constituting a so-called "molecular gate". ZK-5-1-K, with the smallest "molecular gate", only permitted the infusion of CO_2 into the pores, whereas ZK-5-4-K, with the largest "gate", allowed infusion of all of the gas molecules; ZK-5-2-K and ZK-5-3-K, with intermediate pore dimensions, gave intermediate results, implying that excess K^+ will almost entirely close the "molecular gate".

From the N_2 adsorption isotherms on ZK-5-*n*-Cs samples (Table 1), we surmised that Cs^+ was adsorbed far away from the windows, and so could not stop the infusion of CH_4. Fig. 3d shows that the CH_4 adsorption capacity varied with no obvious order. Nevertheless, a further interesting phenomenon was noted: less Cs^+ led to less CH_4 adsorption; in other words, Cs^+ increased the CH_4 uptake capacity between Si/Al = 3.36 and 3.57; as for K^+, too much Cs^+ can also partially block the channels of ZK-5-1-Cs (Si/Al = 3.17), even though it is not adsorbed near the windows. Fig. 4 shows the GCMC calculated results, which corroborated that extra-framework K^+ and Cs^+ cations reside in different sites in ZK-5. K^+ is stably adsorbed near the eight-membered-ring windows(all K^+ cations invariably reside at the centers of the openings). In contrast, Cs^+ resides in the interior regions or outside (unfixed, most of the Cs^+ does not reside at the centers of the openings). Similar conditions are present in ZK-5-1-K and ZK-5-1-Cs samples (Fig. S7), but K^+ stops more larger molecules from diffusing into the

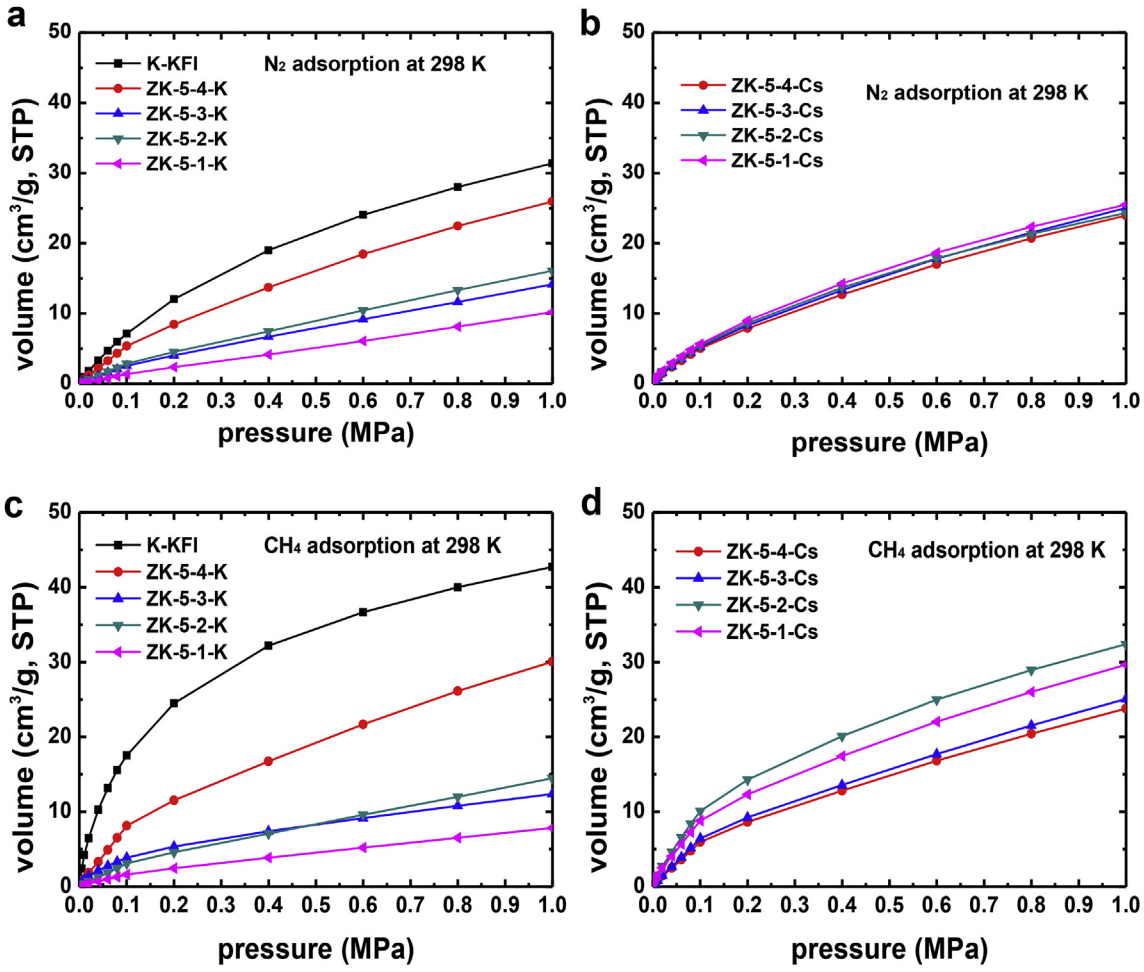

Fig. 3. N_2 and CH_4 adsorption on K-KFI (a, c), ZK-5-N-K (a, c) and ZK-5-N-Cs (b, d) at 298 K and the pressure up to 1 MPa.

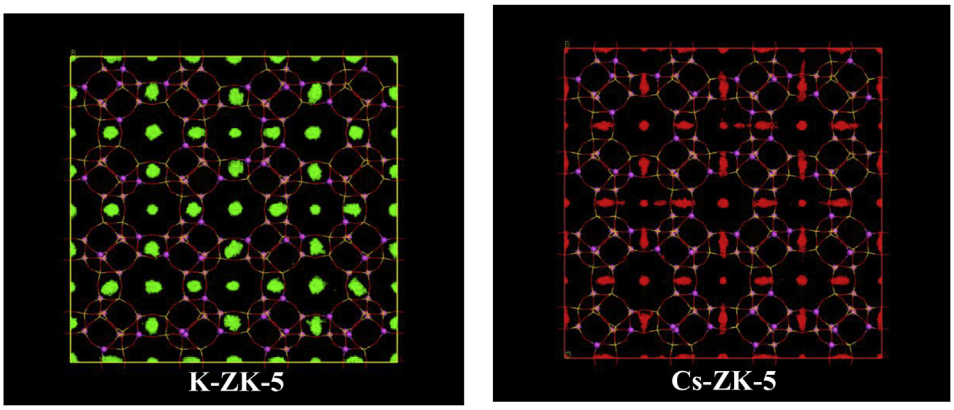

Fig. 4. The position of K and Cs in K-ZK-5 (only K^+ as the balance ion) and Cs-ZK-5(only Cs^+ as the balance ion) was calculated by GCMC method.

pores of the former.

To assess the potential for CO_2 capture from natural gas and biogas on the "molecular gate" zeolite ZK-5, the effect of the number of Cs^+ cations per unit cell of ZK-5 on CO_2/CH_4 (30%/70%, 5%/95%, and 2%/98%) adsorption selectivity was calculated by IAST theory (method description in the SI). The results are shown in Fig. 5. Consistent with the "molecular gate" influence, sample ZK-5-1-K with the lowest Si/Al ratio showed the highest selectivity for CO_2 at either 2%, 5%, or 30%, and the selectivity increased with increasing CO_2 content to a value of 5×10^4, higher than in most literature reports. When K^+ was replaced by Cs^+, the "molecular gate" phenomenon disappeared. ZK-5-Cs samples showed lower selectivity than ZK-5-K samples, because CH_4 could readily infuse into ZK-5-*n*-Cs. The CO_2 selectivity depends only on the surface effect. The quantity of CO_2 taken up from the CO_2/CH_4 mixture was the most important evaluation criterion, which was calculated by IAST theory. The results are shown in Fig. 6. It can be seen that the

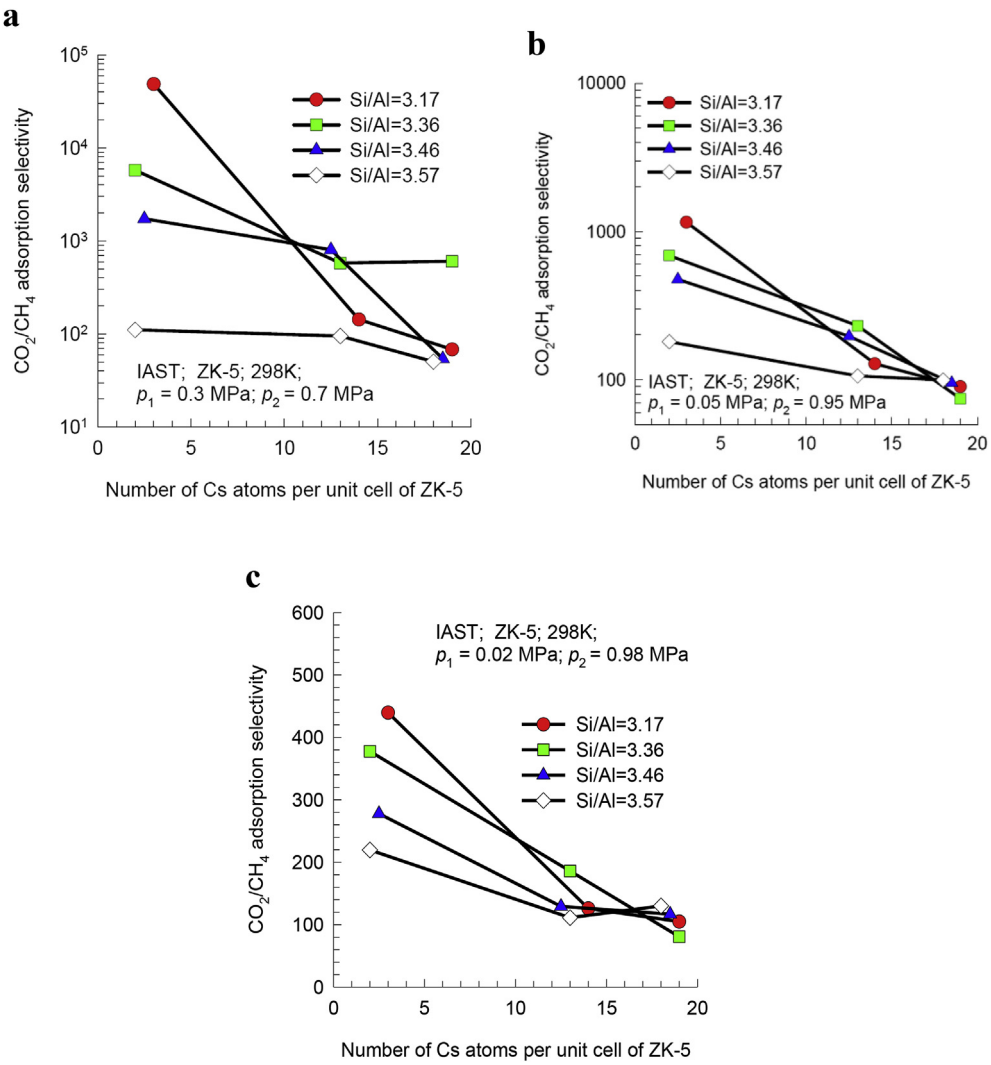

Fig. 5. CO_2/CH_4 (30%/70% (a), 5%/95% (b) and 2%/98% (c)) adsorption selectivity of ZK-5 samples at 1 MPa.

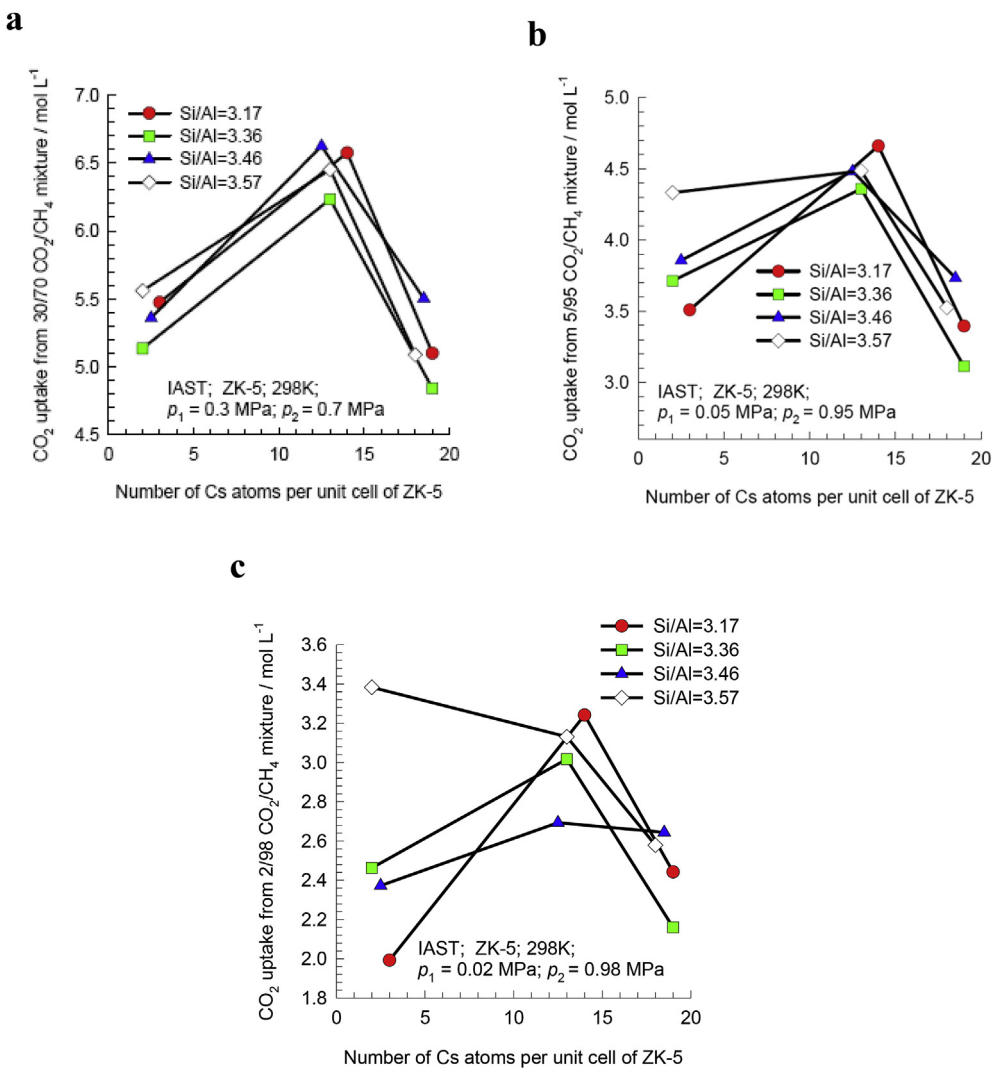

Fig. 6. Volumetric CO_2 uptake from CO_2/CH_4 mixture (30%/70% (a), 5%/95% (b) and 2%/98% (c)) on ZK-5 samples at 1 MPa.

original ZK-5-*n* samples showed higher uptakes than ZK-5-K and ZK-5-Cs when the content of CO_2 was more than 5%, consistent with the single-component adsorption capacities of the ZK-5 samples.

Since the adsorption selectivities of CO_2 over CH_4 and N_2 were very high (> 100) in all the ZK-5 samples in this work, we know the separations were not only influenced by selectivity but also the capacity, so there was no need to aim for a higher selectivity. However, when the CO_2 content was decreased to 2%, a secondary trend seemed to arise, and higher selectivity became the key factor for CO_2 capture uptake. Figs. 5c and 6c indicate thatZK-5-4-K (few Cs^+, white diamonds) showed higher CO_2/CH_4 selectivity and higher CO_2 uptake than ZK-5-4or ZK-5-4-Cs. Thus, high selectivity is the most important factor for the removal of low concentrations of CO_2 ($< 2\%$), as in the decarbonization of natural gas, for instance LNG preparation, which needs a CO_2 concentration < 50 ppm.

In contrast to CO_2 capture from CO_2/CH_4 mixtures, Cs^+ had no regulatory effect on the CO_2/N_2 (15%/85%) adsorption selectivity on ZK-5 at low pressure (100 kPa) compared with K^+ (Fig. 7a). N_2 adsorption capacity was significantly affected by Si/Al ratio, but the total uptake volume was only around 5 $cm^3 g^{-1}$, much less than the CO_2 adsorption at low pressure. From this, we can infer that the CO_2 adsorption volume was the key factor for CO_2/N_2 adsorption selectivity; for instance, ZK-5-4-K showed the highest adsorption capacity according to both the adsorption isotherm and the IAST calculated results (Fig. 7b). Fig. 7b shows another unexpected result in that the quantities of CO_2 taken up from CO_2/N_2 on ZK-5-1/2/3-Cs were higher than those on ZK-5-1/2/3-K, implying that for similar adsorption selectivities, the separations will be influenced by the single composite adsorption capacity.

In order to take proper account of both the selectivity and the CO_2 uptake capacity, we carried out transient breakthrough simulations in fixed-bed adsorbers. Fig. 8 presents a comparison of CO_2 capture capacities for separations of CO_2/CH_4 and CO_2/N_2 mixtures in fixed-bed adsorbers packed with 12 different ZK-5 materials. The CO_2capture capacities show the same dependences on the number of Cs atoms in the framework as observed in Figs. 6 and 7b for the IAST calculations of volumetric CO_2 uptake capacities. There is a precise linear dependence between the two sets of data. This indicates that the separation performance in fixed beds depends primarily on the volumetric CO_2 uptake capacities, except at the low CO_2 concentration of 2%.

5. Conclusions

Since the environmental concerns, capture CO_2 from the flue gas will reduce the global carbon emissions; additionally, CO_2 separation from CH_4 is important in natural gas processing because CO_2 reduces the energy content of natural gas. So, high efficiency adsorbent for carbon capture and decarbonization was very important for the clean energy industry. By adjusting the ratio of the starting materials, we obtained four different ZK-5 samples with Si/Al ratios of 3.17, 3.36,

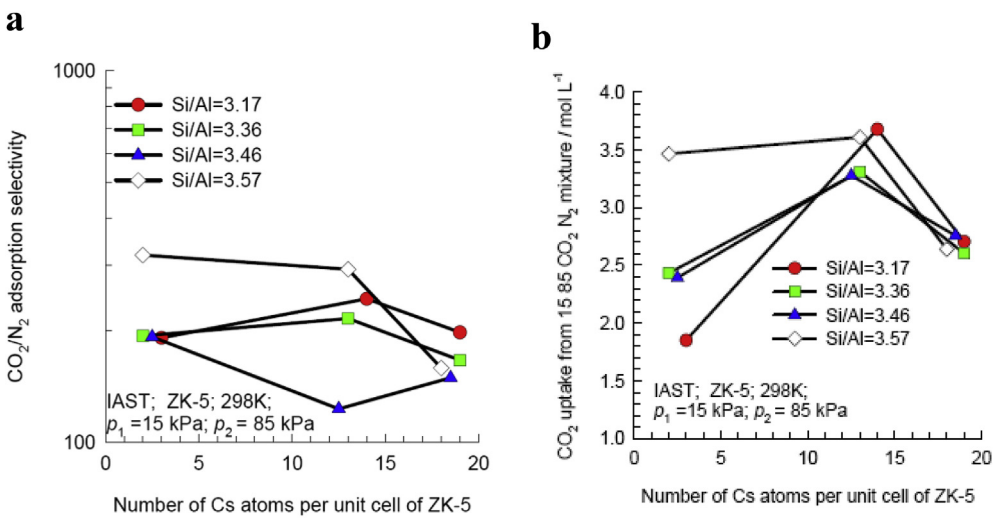

Fig. 7. CO_2/N_2 (15%/85%) adsorption selectivity (a) and volumetric CO_2 uptake from CO_2/N_2 mixture on ZK-5 samples at 100 kPa (b).

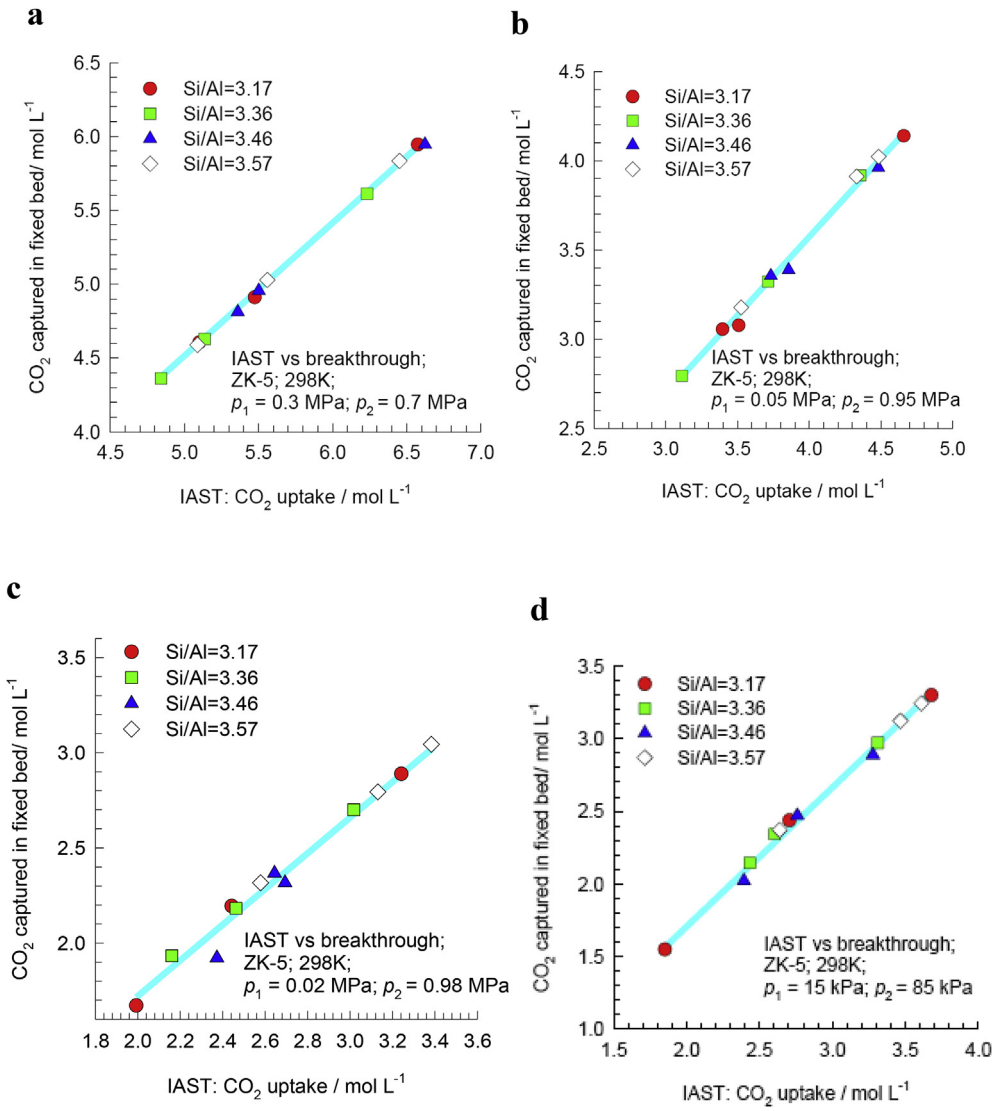

Fig. 8. Comparison of CO_2 capture capacities for separation of 30%/70% (a), 5%/95% (b) and 2%/98% (c) CO_2/CH_4 and 15%/85% (d) CO_2/N_2 mixtures in fixed bed adsorbers packed with 12 different ZK-5 materials (IAST vs breakthrough).

3.46, and 3.57, doped with K^+ or Cs^+ cations. No organic template was necessary in the synthetic process. We found that in the ZK-5-K samples with lower Si/Al ratio (Si/Al < 3.6), excess K^+ cations play a blocking role. Adjustment of the Si/Al ratio yielded a small "molecular gate" adsorbent that prevents the infusion of larger molecules such as CH_4 and N_2, but allows the smaller CO_2 to enter. GCMC results implied that extra-framework K^+ and Cs^+ cations reside in different sites in the ZK-5; K^+ is stably adsorbed near the eight-membered-ring windows, where as Cs^+ resides in the interior regions. The separation performances of 12 different ZK-5 structures have been investigated, with varying Si/Al ratios and varying proportions of extra-framework K^+ and Cs^+ cations. Specifically, the following four sets of separations were examined: 30%/70%, 5%/95%, and 2%/98% CO_2/CH_4 mixtures at a total pressure of 1 MPa, and a 15%/85% CO_2/N_2 mixture at a total pressure of 100 kPa. Both experimental and simulation studies of selectivity and CO_2 uptake have shown that since the adsorption selectivities are in all cases very high (1×10^2–1×10^5), the separations are not influenced by selectivity, and there is no need to aim for high selectivity. However, when the CO_2 content was decreased to 2%, a secondary trend seemed to arise: higher selectivity became the key factor for CO_2 uptake, and hence the prime concern for removal of low CO_2 concentrations (< 2%). This should make the material very suitable for the decarbonization of natural gas, as, for instance, in LNG preparation.

Acknowledgments

We gratefully acknowledge the financial support from the National Natural Science Foundation of China (No.51672186, 21676175), Coal-Based Key Scientific and Technological Project of Shanxi Province, China (No.MQ2014-10).

Appendix A. Supplementary data

Supplementary data related to this article can be found at http://dx.doi.org/10.1016/j.micromeso.2018.03.034.

References

[1] M.E. Boot-Handford, J.C. Abanades, E.J. Anthony, M.J. Blunt, S. Brandani, N. Mac Dowell, J.R. Fernandez, M.C. Ferrari, R. Gross, J.P. Hallett, R.S. Haszeldine, P. Heptonstall, A. Lyngfelt, Z. Makuch, E. Mangano, R.T.J. Porter, M. Pourkashanian, G.T. Rochelle, N. Shah, J.G. Yao, P.S. Fennell, Carbon capture and storage update, Energy Environ. Sci. 7 (2014) 130–189.
[2] S. Choi, J.H. Drese, C.W. Jones, Adsorbent materials for carbon dioxide capture from large anthropogenic point sources, Chem. Sus. Chem. 2 (9) (2009) 796–854.
[3] B. HubbardNew and Emerging Technologies (Petroskills workshop), Gas Processors Association Convention, John M. Campbell & Co, Austin, Texas, 2010.
[4] N. MacDowell, N. Florin, A. Buchard, J. Hallett, A. Galindo, G. Jackson, C.S. Adjiman, C.K. Williams, N. Shah, P. Fennell, An overview of CO2 capture technologies, Energy Environ. Sci. 3 (11) (2010) 1645–1669.
[5] T.E. Rufford, S. Smart, G.C.Y. Watson, B.F. Graham, J. Boxall, J.C. Diniz da Costa, E.F. May, The removal of CO2 and N2 from natural gas: a review of conventional and emerging process technologies, J. Petrol. Sci. Eng. 94–95 (2012) 123–154.
[6] B.T. Kelley, J.A. Valencia, P.S. Northrop, C.J. Mart, Controlled Freeze Zone™ for developing sour gas reserves, Energy Procedia 4 (2011) 824–829.
[7] S.P. Reynolds, A.D. Ebner, J.A. Ritter, Carbon dioxide capture from flue gas by pressure swing adsorption at high temperature using a K-promoted HTlc: effects of mass transfer on the process performance, Environ. Prog. 25 (4) (2006) 334–342.
[8] S. Cavenati, C.A. Grande, A.E. Rodrigues, Removal of carbon dioxide from natural gas by vacuum pressure swing adsorption, Energy Fuel. 20 (6) (2006) 2648–2659.
[9] O. Cheung, N. Hedin, Zeolites and related sorbents with narrow pores for CO 2 separation from flue gas, RSC Adv. 4 (28) (2014) 14480–14494.
[10] N.K. Jensen, T.E. Rufford, G. Watson, D.K. Zhang, K.I. Chan, E.F. May, Screening zeolites for gas separation applications involving methane, nitrogen, and carbon dioxide, J. Chem. Eng. Data 57 (1) (2011) 106–113.
[11] P.J.E. Harlick, F.H. Tezel, Adsorption of carbon dioxide, methane and nitrogen: pure and binary mixture adsorption for ZSM-5 with SiO 2/Al 2 O 3 ratio of 280(J), Separ. Purif. Technol. 33 (2) (2003) 199–210.
[12] O. Cheung, D. Wardecki, Z. Bacsik, P. Vasiliev, L.B. McCuskerad, N. Hedin, Highly selective uptake of carbon dioxide on the zeolite |Na10.2KCs0.8|-LTA – a possible sorbent for biogas upgrading, Phys. Chem. Chem. Phys. 18 (24) (2016) 16080–16083.
[13] O. Cheung, Z. Bacsik, Q. Liu, A. Mace, N. Hedin, Adsorption kinetics for CO2 on highly selective zeolites NaKA and nano-NaKA, Appl. Energy 112 (4) (2013) 1326–1336.
[14] S. Walspurger, L. Boels, P.D. Cobden, G.D. Elzinga, W.G. Haije, R.W. Brink, The crucial role of the K+ aluminium oxide interaction in K+ promoted alumina and hydrotalcite based materials for CO2 sorption at high temperatures, Chem. Sus. Chem. 1 (7) (2008) 643–650.
[15] I.A.A.C. Esteves, M.S.S. Lopes, P.M.C. Nunes, J.P.B. Mota, Adsorption of natural gas and biogas components on activated carbon, Separ. Purif. Technol. 62 (2) (2008) 281–296.
[16] H. Yi, F. Li, P. Ning, X. Tang, J. Peng, Y. Lia, H. Deng, Adsorption separation of CO 2, CH 4, and N 2 on microwave activated carbon, Chem. Eng. J. 215 (2013) 635–642.
[17] B. Yuan, J. Wang, Y. Chen, X. Wu, H. Luo, S. Deng, Unprecedented performance of N-doped activated hydrothermal carbon towards C2H6/CH4, CO2/CH4, and CO2/H2 separation, J. Mater. Chem. 4 (6) (2016) 2263–2276.
[18] J. Wang, R. Krishna, T. Yang, S. Deng, Nitrogen-rich microporous carbons for highly selective separation of light hydrocarbons, J. Mater. Chem. 4 (36) (2016) 13957–13966.
[19] A.C. Kizzie, A.G. Wong-Foy, A.J. Matzger, Effect of humidity on the performance of microporous coordination polymers as adsorbents for CO2 capture, Langmuir 27 (10) (2011) 6368–6373.
[20] J.-R. Li, Y. Ma, M.C. McCarthy, J. Sculley, J. Yu, H. Jeong, P.B. Balbuena, H.C. Zhou, Carbon dioxide capture-related gas adsorption and separation in metal-organic frameworks, Coord. Chem. Rev. 255 (15) (2011) 1791–1823.
[21] P. Mishra, S. Mekala, F. Dreisbach, B. Mandala, S. Gumma, Adsorption of CO2, CO, CH4 and N2 on a zinc based metal organic framework, Separ. Purif. Technol. 94 (2012) 124–130.
[22] J.-R. Li, J. Sculley, H.-C. Zhou, Metal–organic frameworks for separations, Chem. Rev. 112 (2) (2012) 869–932.
[23] M. Moliner, C. Martínez, A. Corma, Synthesis strategies for preparing useful small pore zeolites and zeotypes for gas separations and catalysis, Chem. Mater. 26 (1) (2013) 246–258.
[24] S.M. Kuznicki, V.A. Bell, S. Nair, M. Tsapatsis, A. Burton, R.F. Lobo, R.M. Jacubinas, S.M. Kuznicki, A titanosilicate molecular sieve with adjustable pores for size-selective adsorption of molecules, Nature 412 (6848) (2001) 720–724.
[25] R. Krishna, J.M. Van Baten, Onsager coefficients for binary mixture diffusion in nanopores, Chem. Eng. Sci. 63 (12) (2008) 3120–3140.
[26] J. Shang, G. Li, R. Singh, Q. Gu, K.M. Nairn, T.J. Bastow, N.V. Medhekar, C.M. Doherty, A.J. Hill, J.Z. Liu, P.A. Webley, Discriminative separation of gases by a "molecular trapdoor" mechanism in chabazite zeolites, J. Am. Chem. Soc. 134 (46) (2012) 19246–19253.
[27] S. Ferdov, Temperature- and vacuum-induced framework contraction of Na-ETS-4, Langmuir 26 (4) (2010) 2684–2687.
[28] T. Remy, S.A. Peter, Tendeloo L. Van, S. Van der Perre, Y. Lorgouilloux, C.E.A. Kirschhock, G.V. Baron, J.F.M. Denayer, Adsorption and separation of CO2 on KFI zeolites: effect of cation type and Si/Al ratio on equilibrium and kinetic properties, Langmuir 29 (16) (2013) 4998–5012.
[29] J. Yang, R. Krishna, L. Li, J. Li, Experiments and simulations on separating a CO2/CH4 mixture using K-KFI at low and high pressures, Microporous Mesoporous Mater. 184 (2014) 21–27.
[30] T. Remy, E. Gobechiya, D. Danaci, S.A. Peter, P. Xiao, L. Van Tendeloo, S. Couck, J. Shang, C.E.A. Kirschhock, R.K. Singh, J.A. Martens, G.V. Baron, P.A. Webley, J.F.M. Denayer, RSC Adv. 4 (107) (2014) 62511–62524.
[31] Q. Liu, T. Pham, M.D. Porosoff, R.F. Lobo, ZK-5: a CO2-selective zeolite with high working capacity at ambient temperature and pressure, Chem. Sus. Chem. 5 (11) (2012) 2237–2242.
[32] T.D. Pham, M.R. Hudson, C.M. Brown, R.F. Lobo, On the structure–property relationships of cation-exchanged ZK-5 zeolites for CO2 adsorption, Chem. Sus. Chem. 10 (5) (2017) 946–957.
[33] J. Yang, Q. Zhao, H. Xu, L. Li, J. Dong, J. Li, Adsorption of CO2, CH4, and N2 on gas diameter grade ion-exchange small pore zeolites, J. Chem. Eng. Data 57 (12) (2012) 3701–3709.
[34] J. P. Verduijn, Zeolite ZK-5: U.S. Patent 4,994,249. (1991-2-19).
[35] G.C. Maitland, M. Rigby, E.B. Smith, W.A. Wakeham, Intermolecular Forces: Their Origin and Determination, Clarendon Press, Oxford, U.K, 1981.
[36] R. Krishna, The maxwell-stefan description of mixture diffusion in nanoporous crystalline materials, Microporous Mesoporous Mater. 185 (2014) 30–50.
[37] R. Krishna, Methodologies for evaluation of metal-organic frameworks in separation applications, RSC Adv. 5 (2015) 52269–52295.
[38] R. Krishna, J.R. Long, Screening metal-organic frameworks by analysis of transient breakthrough of gas mixtures in a fixed bed adsorber, J. Phys. Chem. C 115 (2011) 12941–12950.
[39] M.M. Dubinin, Microporous structures and absorption properties of carbonaceous adsorbents, Carbon 21 (1983) 359–366.
[40] F. Carrasco-Marin, M.V. López-Ramón, C. Moreno-Castilla, Applicability of the dubinin-radushkevich equation to CO2 adsorption on activated carbons, Langmuir 9 (1993) 2758–2760.

ESI (Electronic Supporting Information)

Adjusting the Proportions of Extra-Framework K^+ and Cs^+ Cations to Construct a "Molecular Gate" on ZK-5 for CO_2 Capture

Jiangfeng Yang[ac],Hua Shang[a], Rajamani Krishna[b], Yong Wang[c], Kun Ouyang[a], Jinping Li[ac]*

[a]Research Institute of Special Chemicals, College of Chemistry and Chemical Engineering, Taiyuan University of Technology, Taiyuan 030024, Shanxi, P. R. China

[b]Van 't Hoff Institute for Molecular Sciences, University of Amsterdam, Science Park 904,1098 XH Amsterdam, The Netherlands

[c] Shanxi Key Laboratory of Gas Energy Efficient and Clean Utilization, Taiyuan 030024, Shanxi, P. R. China

Table S1. ZK-5 structural properties.

Structural formula of ZK-5 for 1 unit cell	Indicative name	ρ kg m^{-3}
$O_{192}Al_{23}Si_{73}K_9Cs_{14}$	ZK-5-1	2060.2
$O_{192}Al_{22}Si_{74}K_9Cs_{13}$	ZK-5-2	2026.1
$O_{192}Al_{21.5}Si_{74.5}K_9Cs_{12.5}$	ZK-5-3	2009.0
$O_{192}Al_{21}Si_{75}K_8Cs_{13}$	ZK-5-4	2016.3
$O_{192}Al_{23}Si_{73}K_{21}Cs_2$	ZK-5-1-K	1768.3
$O_{192}Al_{22}Si_{74}K_{20}Cs_2$	ZK-5-2-K	1758.9
$O_{192}Al_{21.5}Si_{74.5}K_{19.5}Cs_2$	ZK-5-3-K	1753.8
$O_{192}Al_{21}Si_{75}K_{19}Cs_2$	ZK-5-4-K	1749.0
$O_{192}Al_{23}Si_{73}K_4Cs_{19}$	ZK-5-1-Cs	2181.7
$O_{192}Al_{22}Si_{74}K_3Cs_{19}$	ZK-5-2-Cs	2182.0
$O_{192}Al_{21.5}Si_{74.5}K_{3.5}Cs_{18.5}$	ZK-5-3-Cs	2159.9
$O_{192}Al_{21}Si_{75}K_3Cs_{18}$	ZK-5-4-Cs	2137.7

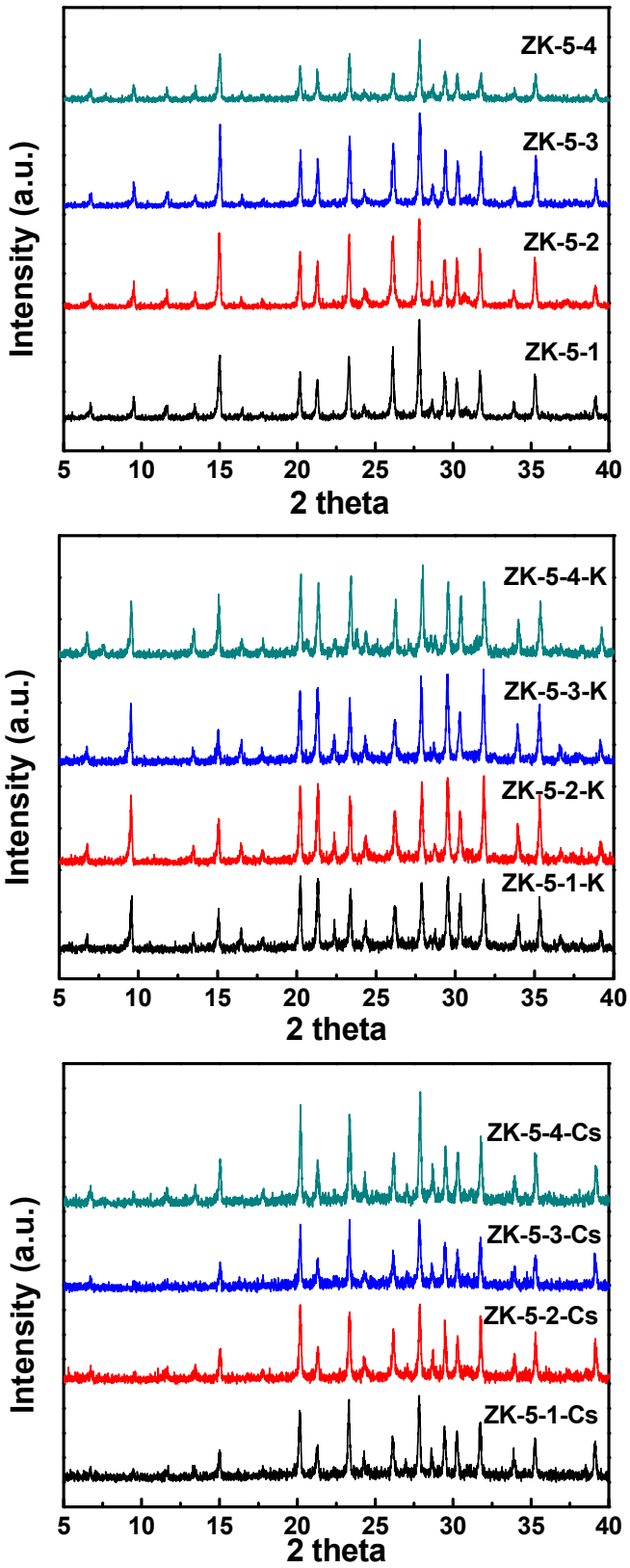

Figure S1. XRD patterns of ZK-5

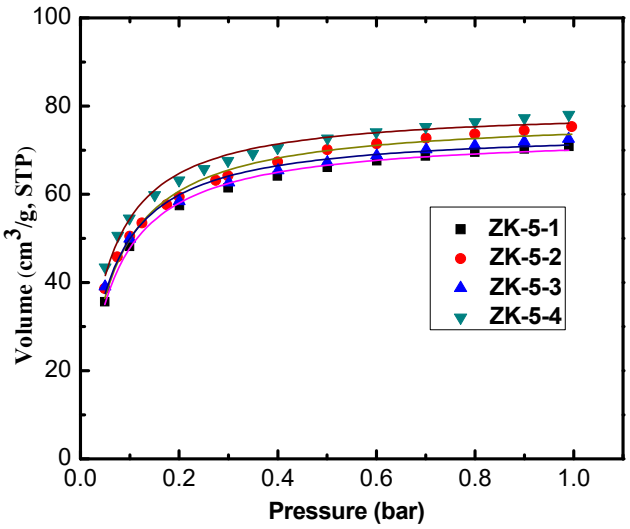

Figure S2.CO_2 adsorption isotherms ZK-5-1/2/3/4 at 273 K

Table S2. The surface area of the samples obtained from CO_2 at 273K

SAMPLES	ZK-5-1	ZK-5-2	ZK-5-3	ZK-5-4
SURFACE AREA (m^2/g)	392	412.16	398.72	426.16

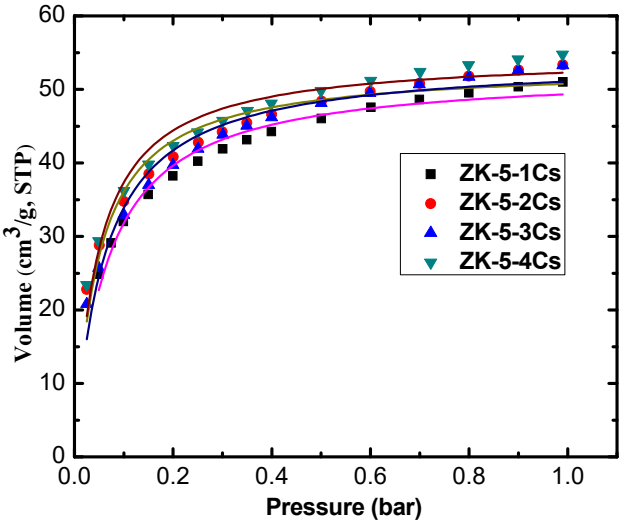

Figure S3. CO_2 adsorption isotherms ZK-5-1/2/3/4-Cs at 273 K

Table S3. The surface area of the samples obtained from CO_2 at 273K

SAMPLES	ZK-5-1Cs	ZK-5-2Cs	ZK-5-3Cs	ZK-5-4Cs
SURFACE AREA (m^2/g)	276.20	284.14	285.82	292.66

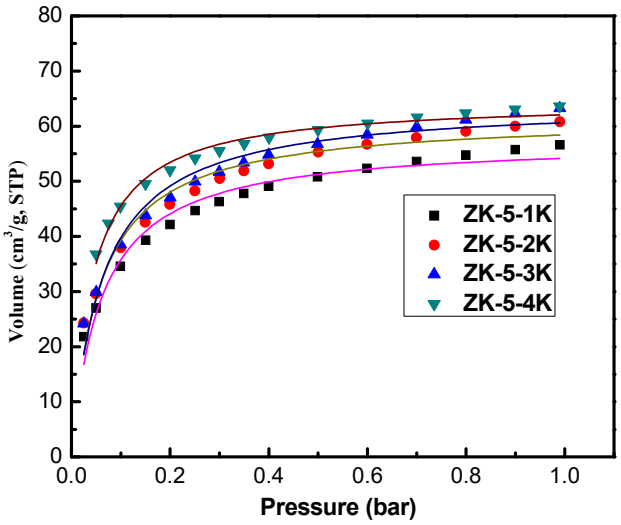

Figure S4. CO_2 adsorption isotherms ZK-5-1/2/3/4-K at 273 K

Table S4. The surface area of the samples obtained from CO_2 at 273K

SAMPLES	ZK-5-1K	ZK-5-2K	ZK-5-3K	ZK-5-4K
SURFACE AREA (m^2/g)	303.24	326.93	339.30	347.31

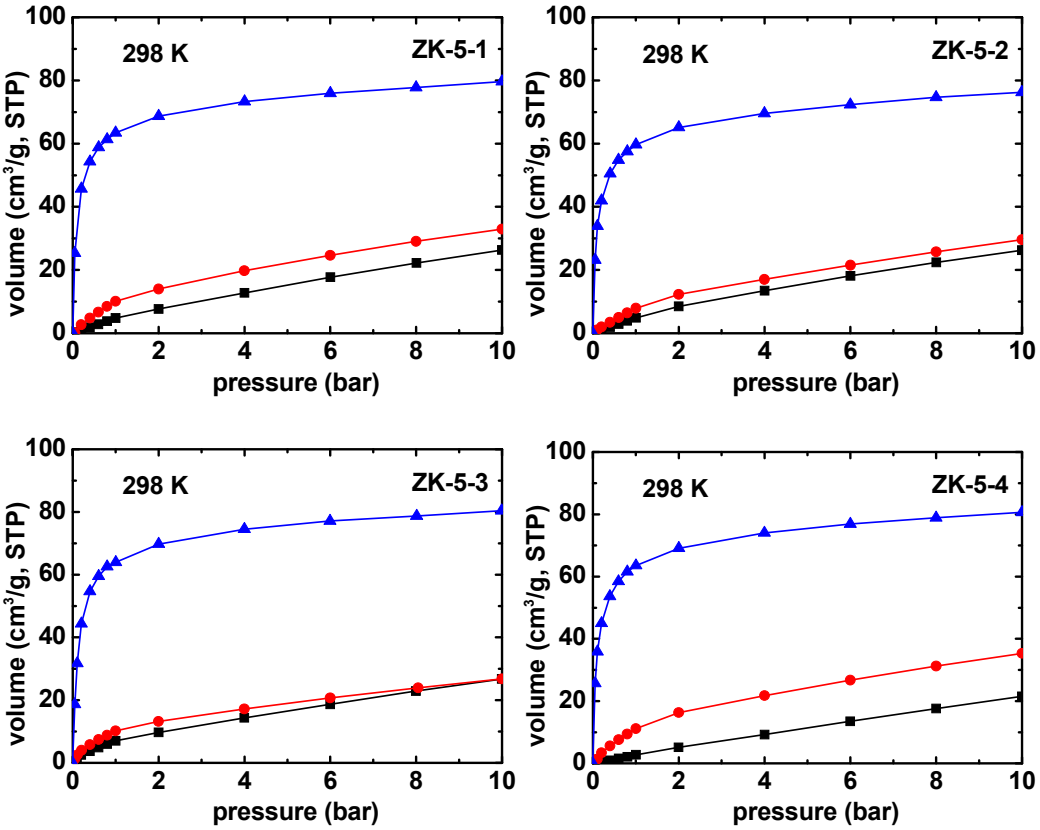

Figure S5. CO_2, CH_4 and N_2 adsorption isothermsof ZK-5-1/2/3/4 at 298 Kand the pressure up to 10 bar

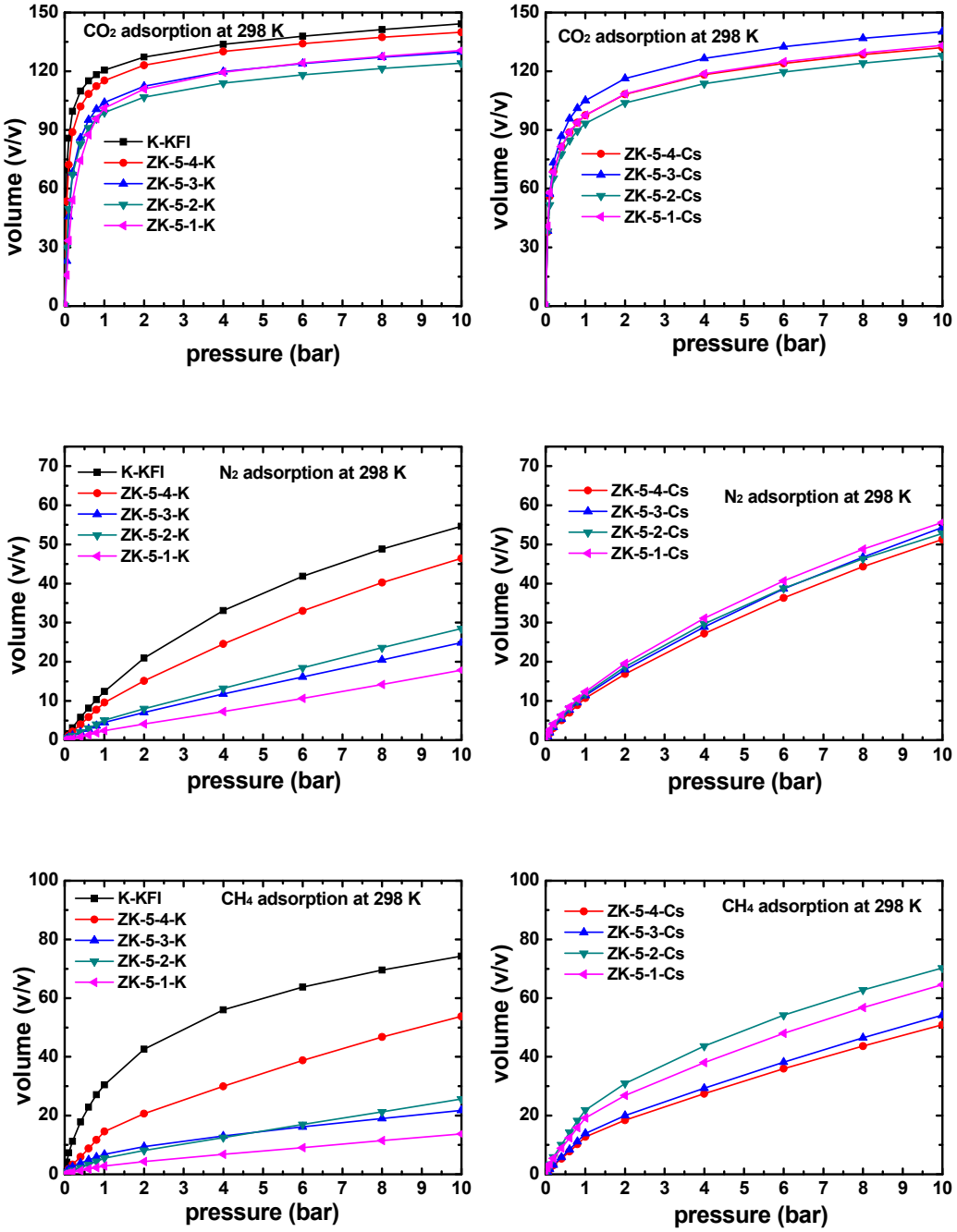

Figure S6. CO_2,CH_4 and N_2 adsorption on K-KFI, ZK-5-N-K and ZK-5-N-Cs at 298 K and the pressure up to 10 bar

Table S5. Langmuir-Freundlich parameters for CO_2 in ZK-5 at 298 K.

Structural formula of ZK-5 for 1 unit cell	Indicative name	q_{sat} mol kg^{-1}	b Pa^{-1}	ν dimensionless
$O_{192}Al_{23}Si_{73}K_9Cs_{14}$	ZK-5-1	3.3	1.171×10^{-3}	0.7
$O_{192}Al_{23}Si_{73}K_{20}Cs_3$	ZK-5-1-K	3.4	2.94×10^{-5}	1
$O_{192}Al_{23}Si_{73}K_4Cs_{19}$	ZK-5-1-Cs	3.2	4.8×10^{-3}	0.51
$O_{192}Al_{22}Si_{74}K_9Cs_{13}$	ZK-5-2	3.6	1.49×10^{-3}	0.66
$O_{192}Al_{22}Si_{74}K_{20}Cs_2$	ZK-5-2-K	3.2	1.81×10^{-4}	0.87
$O_{192}Al_{22}Si_{74}K_3Cs_{19}$	ZK-5-2-Cs	3	4.54×10^{-3}	0.52
$O_{192}Al_{21.5}Si_{74.5}K_9Cs_{12.5}$	ZK-5-3	3.65	3.19×10^{-4}	0.82
$O_{192}Al_{21.5}Si_{74.5}K_{19}Cs_{2.5}$	ZK-5-3-K	3.25	4.88×10^{-5}	1
$O_{192}Al_{21.5}Si_{74.5}K_{3.5}Cs_{18.5}$	ZK-5-3-Cs	3.2	1.75×10^{-3}	0.62
$O_{192}Al_{21}Si_{75}K_8Cs_{13}$	ZK-5-4	3.8	1.91×10^{-3}	0.64
$O_{192}Al_{21}Si_{75}K_{19}Cs_2$	ZK-5-4-K	3.6	2.65×10^{-3}	0.64
$O_{192}Al_{21}Si_{75}K_3Cs_{18}$	ZK-5-4-Cs	3.04	2.64×10^{-3}	0.58

Table S6. Langmuir-Freundlich parameters for CH_4 in ZK-5 at 298 K.

Structural formula of ZK-5 for 1 unit cell	Indicative name	q_{sat} mol kg^{-1}	b Pa^{-1}	ν dimensionless
$O_{192}Al_{23}Si_{73}K_9Cs_{14}$	ZK-5-1	3.2	2.56×10^{-5}	0.75
$O_{192}Al_{23}Si_{73}K_{20}Cs_3$	ZK-5-1-K	0.85	1.99×10^{-6}	0.92
$O_{192}Al_{23}Si_{73}K_4Cs_{19}$	ZK-5-1-Cs	3.2	2.17×10^{-5}	0.75
$O_{192}Al_{22}Si_{74}K_9Cs_{13}$	ZK-5-2	1.85	6.18×10^{-6}	0.91
$O_{192}Al_{22}Si_{74}K_{20}Cs_2$	ZK-5-2-K	1.2	1.04×10^{-6}	1
$O_{192}Al_{22}Si_{74}K_3Cs_{19}$	ZK-5-2-Cs	2.2	7.93×10^{-6}	0.89
$O_{192}Al_{21.5}Si_{74.5}K_9Cs_{12.5}$	ZK-5-3	1.72	8.88×10^{-5}	0.71
$O_{192}Al_{21.5}Si_{74.5}K_{19}Cs_{2.5}$	ZK-5-3-K	1.8	7.05×10^{-5}	0.63
$O_{192}Al_{21.5}Si_{74.5}K_{3.5}Cs_{18.5}$	ZK-5-3-Cs	7.8	1.04×10^{-5}	0.7
$O_{192}Al_{21}Si_{75}K_8Cs_{13}$	ZK-5-4	4.1	5.03×10^{-6}	0.68
$O_{192}Al_{21}Si_{75}K_{19}Cs_2$	ZK-5-4-K	6.1	1.53×10^{-5}	0.71
$O_{192}Al_{21}Si_{75}K_3Cs_{18}$	ZK-5-4-Cs	10	7.44×10^{-5}	0.7

Table S7. Langmuir-Freundlich parameters for N_2 in ZK-5 at 298 K.

Structural formula of ZK-5 for 1 unit cell	Indicative name	q_{sat} mol kg^{-1}	b Pa^{-1}	ν dimensionless
$O_{192}Al_{23}Si_{73}K_9Cs_{14}$	ZK-5-1	3	6.23×10^{-7}	1
$O_{192}Al_{23}Si_{73}K_{20}Cs_3$	ZK-5-1-K	4.2	1.2×10^{-7}	1
$O_{192}Al_{23}Si_{73}K_4Cs_{19}$	ZK-5-1-Cs	2	1.27×10^{-6}	1
$O_{192}Al_{22}Si_{74}K_9Cs_{13}$	ZK-5-2	3	6.35×10^{-7}	1
$O_{192}Al_{22}Si_{74}K_{20}Cs_2$	ZK-5-2-K	6	1.12×10^{-6}	0.85
$O_{192}Al_{22}Si_{74}K_3Cs_{19}$	ZK-5-2-Cs	5.7	9.83×10^{-6}	0.73
$O_{192}Al_{21.5}Si_{74.5}K_9Cs_{12.5}$	ZK-5-3	8	1.63×10^{-5}	0.67
$O_{192}Al_{21.5}Si_{74.5}K_{19}Cs_{2.5}$	ZK-5-3-K	8	1.33×10^{-6}	0.8
$O_{192}Al_{21.5}Si_{74.5}K_{3.5}Cs_{18.5}$	ZK-5-3-Cs	9.4	4.89×10^{-6}	0.74
$O_{192}Al_{21}Si_{75}K_8Cs_{13}$	ZK-5-4	8.5	1.28×10^{-7}	1
$O_{192}Al_{21}Si_{75}K_{19}Cs_2$	ZK-5-4-K	5.7	4.04×10^{-6}	0.8
$O_{192}Al_{21}Si_{75}K_3Cs_{18}$	ZK-5-4-Cs	7.8	5.01×10^{-6}	0.75

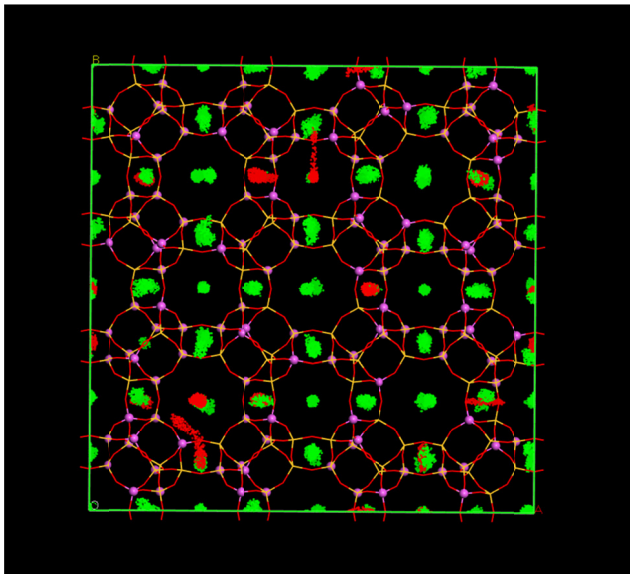

ZK-5-1-K (K/Cs=152/24)

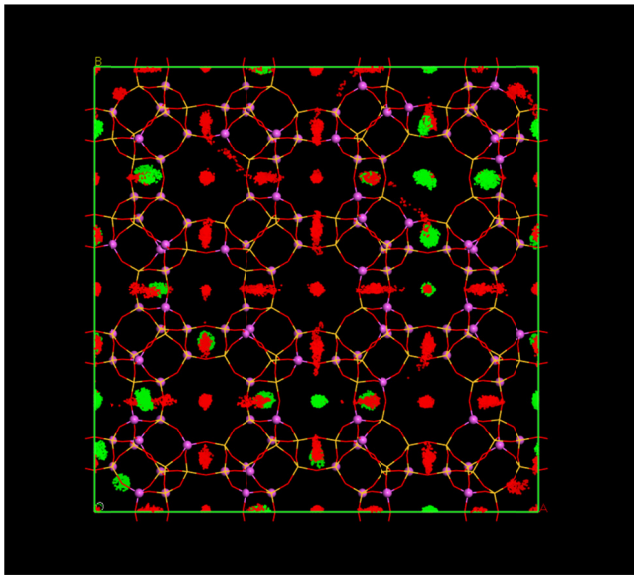

ZK-5-1-Cs (K/Cs=28/148)

Figure S7. The position of K and Cs in ZK-5-K-1 and ZK-5-Cs-1 (Red dot: moving trajectory of Cs^{+}) (Green dot: moving trajectory of K^{+}).

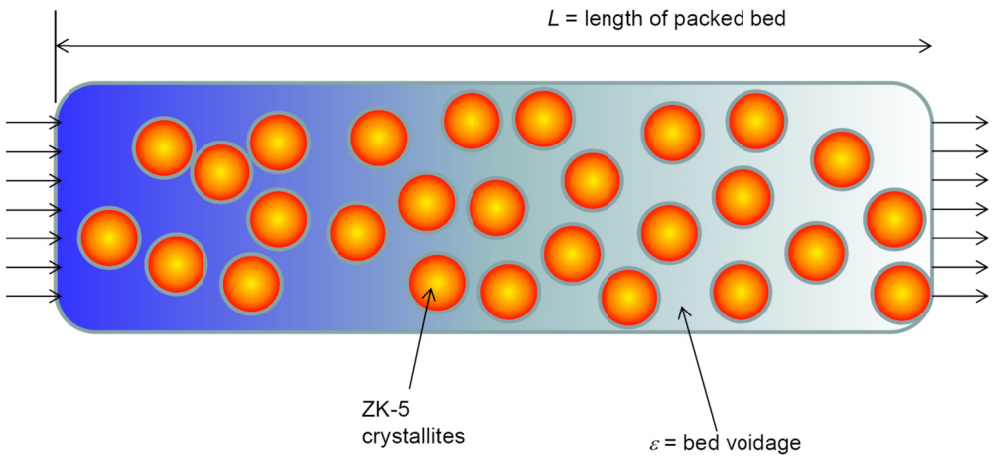

Figure S8. Schematic of a packed bed adsorber.

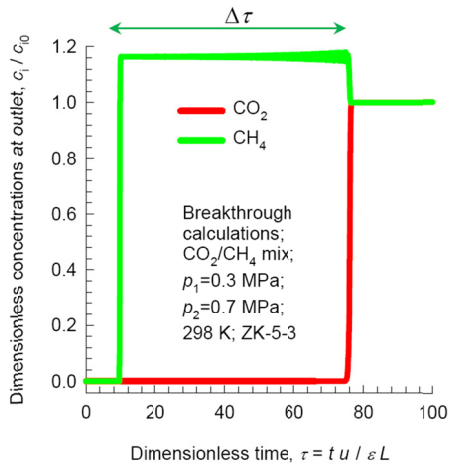

Figure S9. Transient breakthrough of 30/70 CO_2/CH_4 mixtures at a total pressure of 1 MPa in a fixed bedpacked with ZK-5-3.